Carbohydrate Polymers 107 (2014) 138–150

Contents lists available at ScienceDirect

Carbohydrate Polymers

journal homepage: www.elsevier.com/locate/carbpol

Activation of intrinsic apoptotic signaling pathway in cancer cells by *Cymbopogon citratus* polysaccharide fractions

Ramar Thangam[a,b], Malairaj Sathuvan[c], Arasu Poongodi[d,b], Veeraperumal Suresh[e], Kalailingam Pazhanichamy[e], Srinivasan Sivasubramanian[b], Nagarajan Kanipandian[g], Nalini Ganesan[d], Ramasamy Rengasamy[c], Ramasamy Thirumurugan[g], Soundarapandian Kannan[a,f,*]

[a] *Proteomics & Molecular Cell Physiology Lab, Department of Zoology, Bharathiar University, Coimbatore, TN, India*
[b] *Department of Virology, King Institute of Preventive Medicine & Research, Chennai, TN, India*
[c] *Centre for Advanced Studies in Botany, University of Madras, Chennai, TN, India*
[d] *Department of Biochemistry, Sri Ramachandra University, Chennai, TN, India*
[e] *Department of Biotechnology, Indian Institute of Technology Madras, Chennai, TN, India*
[f] *Department of Zoology, Periyar University, Salem, TN, India*
[g] *Department of Animal Science, Bharathidasan University, Tiruchirapalli, TN, India*

ARTICLE INFO

Article history:
Received 19 July 2013
Received in revised form 6 February 2014
Accepted 7 February 2014
Available online 20 February 2014

Keywords:
Cymbopogon citratus
Plant polysaccharide
Xylofuranose
Cancer cells
Cytotoxicity
Gene expression
Intrinsic apoptotic pathway

ABSTRACT

Essential oils of *Cymbopogon citratus* were already reported to have wide ranging medical and industrial applications. However, information on polysaccharides from the plant and their anticancer activities are limited. In the present study, polysaccharides from *C. citratus* were extracted and fractionated by anion exchange and gel filtration chromatography. Two different polysaccharide fractions such as F1 and F2 were obtained, and these fractions were found to have distinct acidic polysaccharides as characterized by their molecular weight and sugar content. NMR spectral analysis revealed the presence of (1→4) linked b-D-Xylofuranose moiety in these polysaccharides. Using these polysaccharide fractions F1 and F2, anti-inflammatory and anticancer activities were evaluated against cancer cells *in vitro* and the mechanism of action of the polysaccharides in inducing apoptosis in cancer cells *via* intrinsic pathway was also proposed. Two different reproductive cancer cells such as Siha and LNCap were employed for *in vitro* studies on cytotoxicity, induction of apoptosis and apoptotic DNA fragmentation, changes in mitochondrial membrane potential, and profiles of gene and protein expression in response to treatment of cells by the polysaccharide fractions. These polysaccharide fractions exhibited potential cytotoxic and apoptotic effects on carcinoma cells, and they induced apoptosis in these cells through the events of up-regulation of caspase 3, down-regulation of bcl-2 family genes followed by cytochrome *c* release.

1. Introduction

The plant *Cymbopogon citratus* (DC) Stapf Poaceae/Gramineae, commonly known as lemongrass, is a spontaneous perennial grass, largely distributed around the world, especially in tropical and subtropical countries. Essential oils of the plant have potential pharmacological and biological activities. Citral, the essential oil of the plant leaf, has applications in food, perfumery, soap, cosmetic, pharmaceutical and insecticide industries (Negrelle & Gomes, 2007). Aqueous extracts of dried leaves are used in traditional medicine for the treatment of inflammation, digestive disorders, diabetes, nervous disorders, cancer, fever, *etc.* (Carbajal, Casaco, Arruzazabala, Gonzalez, & Tolon, 1989; Costa et al., 2011; Francisco et al., 2011; Lorenzetti, Souza, Sarti, Filho, & Ferreira, 1991). However, studies on chemical characterization of the plant polysaccharides and their bioactive properties such as anti-inflammatory and anticancer activities are not reported.

Tumor cell death by most anti-cancer strategies has been linked to the activation of apoptosis signal transduction pathways in cancer cells involving intrinsic and/or extrinsic pathway, and the pathways are activated through mitochondria or a cell surface

* Corresponding author at: Proteomics & Molecular Cell Physiology Lab, Department of Zoology, Bharathiar University, Coimbatore, TN, India.
Tel.: +91 422 2428310; fax: +91 422 2425706; mobile: +91 9486252052.
E-mail addresses: thangam1985@yahoo.co.in (R. Thangam), sk.protein@buc.edu.in, skperiyaruniv@gmail.com (S. Kannan).

http://dx.doi.org/10.1016/j.carbpol.2014.02.039
0144-8617/

receptor. The mitochondrial-mediated intrinsic apoptotic pathway is activated by a mitochondrial derived death signal, leading to the expression of several mitochondrial genes such as bax, bcl-2, p53 and cox-2 resulting in the release of cytochrome *c* from the mitochondrial inter-membrane space into the cytosol. The released cytochrome *c* binds to Apaf-1 and activates pro-caspase 9, which resulted in the activation of caspase 3 and other effector caspases. It has been reported that p53 can act as a trans-activator or repressor for a set of pro- or anti-apoptotic genes. DNA damage is a common event in life following which, the repair mechanisms and apoptosis will be initiated. The tumor-suppressor protein p53 provides an important link between DNA damage and apoptosis (Zhao et al., 2013).

This study aims to explore the anticancer properties of *C. citratus* polysaccharide fractions by addressing the mechanism of action in induction of mitochondrial mediated apoptosis. Here, we have elucidated cytotoxicity as well as the cellular mechanism of intrinsic apoptosis in human cancer cells such as Siha (cervical cancer) and LNCap (prostate cancer). Semi-quantitative Reverse Transcription PCR (RT-PCR) and Western blotting analysis were performed to quantify the expression of genes and proteins involved in intrinsic apoptotic pathway. In this study, mitochondrial mediated apoptosis was found to be accompanied by the events such as alteration in the expression of the bcl-2 family members, disruption of mitochondrial membrane potential, release of cytochrome *c* from mitochondria and activation of downstream caspase 3 by cleavage. The findings of the study will be helpful not only to understand the antitumor mechanism of polysaccharides but also facilitate attempts on developing polysaccharide based novel antitumor agents.

2. Materials and methods

2.1. Materials

The selected cancer cell lines such as Siha and LNCap were cultured in Eagles and RPMI 1640 medium, respectively. MTT [3-(4,5-dimethylthiazol-2-yl)-2,5-diphenyl tetrazolium bromide] was purchased from Hi-Media Laboratories, India. Dimethyl sulfoxide, TriZol Reagent, Rhodamine 123 and HOECHST 33342 were sourced from Sigma Aldrich, USA. cDNA Synthesis Kit (SuPrime Script RT Master Mix, Cat#SR2000) was purchased from GeNetBio, Korea. Antibodies against cytochrome *c* and Caspase 3 were purchased from Santa Cruz Biotechnology, Inc. (Santa Cruz, CA). Antibody against β-actin was purchased from Bio-world (St. Louis Park, MN, USA). Horseradish peroxidase-conjugated secondary antibodies were purchased from Jackson Immuno Research (West Grove, PA, USA). All other reagents and chemicals were of the highest purity grade.

2.2. Extraction of polysaccharides from C. citratus

The leaves of *C. citratus* were collected and shade dried for 7 days at ambient temperature and powdered. Briefly, the shade dried leaves were ground to pieces of about 1 mm diameter. A total of 500 g of leaf powder (dry biomass) was soaked separately in chloroform–methanol solvent system (1:2) for two days in a shaker at 200 rpm (REMI, Mumbai). The process was repeated twice to ensure complete de-coloration and de-fatting of dry biomass. This biomass was dried into a powder and boiled in 1 L of Milli-Q water at 100 °C for 2 h. The pellet was re-extracted as stated above, and the supernatants were pooled. The resulting supernatant was kept at 4 °C overnight and precipitated with two volumes of absolute ethanol 1:2 (v:v). The precipitate was collected, dissolved in water and dialyzed against water using a membrane (MWCO 14,000, Hi-Media, India) at 4 °C for two days; the dialysate was then freeze dried. The detailed steps involved in the extraction, optimization and its preliminary characterization of polysaccharides from the *C. citratus* are already reported by Thangam, Suresh, and Kannan (2014).

2.3. Purification of polysaccharides by anion exchange chromatography

Crude polysaccharides dissolved in Milli-Q water were applied to a column of DEAE-Cellulose 52 (Genei, Bangalore, India) (3 cm × 30 cm), followed by collection of fractions with linear gradient elution using 0–1 M sodium chloride at a flow rate of 60 mL/h eluent (5 mL/tube), and the carbohydrate content was determined by phenol–sulfuric acid method using xylose as the standard (Dubois, Gilles, Hamilton, Rebers, & Smith, 1956). All the active polysaccharide rich fractions were dialyzed against water and lyophilized for further study. The total sugar content was determined using the phenol–sulfuric acid method (Dubois et al., 1956). Total uronic acid content was analyzed colorimetrically by m-phenylphenol method using glucuronic acid as standard (Filisetti-Cozzi & Carpita, 1991).

2.4. Monosaccharide determination

To determine the neutral sugar composition of polysaccharide fractions, the samples (5 mg each) were added to 4 mL of 100% trifluoroacetic acid (TFA) in a round-bottom flask. The mixtures were left overnight at ambient temperature and refluxed for 2 h. The solutions were then diluted to 80% TFA using de-ionized water and refluxed for 30 min. The solutions were diluted again to 30% TFA using de-ionized water and refluxed for 4 h. The TFA was removed using a rotary vacuum evaporator. The solids were washed with de-ionized water and the remaining water was re-evaporated. This procedure was repeated several times until the hydrolysates became neutral. The hydrolysates were derivatized with 450 μL 1-phenyl-3-methyl-5-pyrazolone (PMP) (0.5 M in methanol) and 450 μL 0.3 M NaOH at 70 °C for 30 min (Lines, 1996; Yang, Zhao, & Wang, 2005). After cooled to room temperature, the derivatives were neutralized with 450 μL 0.3 M hydrochloric acid (HCl), and extracted three times with 1 mL chloroform to remove the excess reagent. The aqueous layer was analyzed directly by Agilant 1100 High Performance Liquid Chromatography (HPLC) (Agilant Technologies, Santa Clara, CA, USA) using a C_{18} column (ZORBAXEclipseXDB-C18, 4.6 mm × 150 mm, 3.5 μm). The flow rate was set to 1 mL/min, the temperature was at 25 °C, and the wavelength for variable wavelength detection was 250 nm. The mobile phases were a mixture of buffers A and B, which were 0.05 M potassium di-hydrogen phosphate (KH_2PO_4, pH 6.9) with 15% and 40% acetonitrile, respectively. A gradient of 8–17% buffer B in 25 min was used for separation (Xin, Zhaohui, Wenjing, & Changhu, 2011).

2.5. Molecular weight analysis

The molecular mass of acidic polysaccharide fractions (F1 and F2) was analyzed by gel filtration chromatography. The purified fractions (5 mg) were applied to the column (90 cm × 1.0 cm) packed with Sepharose 6B, and the constituents of the fractions were eluted using 100 mM sodium phosphate buffer (pH 7.2) as the eluent with the flow rate of 0.6 mL/min. The fractions of 2 mL were collected and checked with a phenol–sulfuric acid reaction (Dubois et al., 1956). Dextrans (500, 70, 40 and 10 kDa) were used as calibration standards for the chromatography experiment.

2.6. FTIR spectral analysis

1 mg of F1 and F2 polysaccharide fractions was mixed with KBr and the FTIR spectrum was recorded in the spectral range of 450–4500 cm^{-1} (Perkin Elmer MPF 44B, Waltham, MA, USA).

2.7. NMR spectral analysis

^{1}H and ^{13}C NMR experiments were performed for F1 and F2 fractions in D_2O at 297 K using a 500 MHz FT NMR spectrometer with the operating frequency of 500.13 MHz.

2.8. Cell culture and maintenance

The selected human cancer cell lines such as Siha and LNCap were maintained in Dulbecco's Modified Eagles Medium (DMEM) and RPMI-1640 medium, respectively with supplementation of 2 mM L-glutamine and Balanced Salt Solution (BSS) adjusted to contain 1.5 g/L Na_2CO_3, 0.1 mM non-essential amino acids, 1 mM sodium pyruvate, 2 mM L-glutamine, 1.5 g/L glucose, 10 mM HEPES and 10% fetal bovine serum (GIBCO, USA). Penicillin and streptomycin (100 IU/100 μg) were added to the medium and adjusted to 1 mL/L. The cells were maintained at 37 °C with 5% CO_2 in a humidified CO_2 incubator for 48 h.

2.9. Cell viability assay

Cell viability was analyzed by 3-(4,5-dimethylthiazol-2-yl)-2,5-di-phenyl-tetrazolium bromide (MTT) assay, as described by Mosman (1983). Briefly, exponentially growing cells (1×10^5 cells/mL) were seeded in 96-well plates and were treated with different concentrations of UF, F1, and F2 in the series of 100–1000 μg/mL for 24, 48 and 72 h with FCS free complete medium. 100 μL of MTT (5 mg/mL) was added to 24, 48 and 72 h treated wells. After the plates were incubated at 37 °C for 4 h, the supernatant was aspirated, and 200 μL of di-methyl sulfoxide (DMSO) was added to each well to dissolve the formosan crystals. Absorbance was measured at 620 nm using a 96-well microplate reader (THERMO Multiskan, USA). The percentage of surviving cells was calculated with the following equation:

$$\text{The ratio of cell viability (\%)} = \frac{\text{Mean absorbance of polysaccharide treated wells}}{\text{Mean absorbance of untreated control wells}} \times 100$$

2.10. HOECHST 33342 staining for nuclear apoptosis

The selected cancer cells were seeded in 6 well plates and maintained at 37 °C with 5% CO_2 in a humidified CO_2 incubator for 48 h. Subsequently, the cells were treated with F1 and F2 polysaccharide fractions with their IC_{50} concentrations obtained in various incubation duration such as 24 h, 48 h and 72 h were selected for this staining. At the indicated times, the medium was removed gently, and the cells were washed twice with phosphate buffered saline (PBS), fixed in 4% para-formaldehyde for 20 min, re-washed, and stained with HOECHST 33342 (10 μg/mL) at 37 °C for 20 min in the dark. Stains were then washed with methanol followed by PBS, and the plate was immediately observed in blue channel fluorescence with fluorescent microscopy (Nikon Eclipse, Inc., Japan).

2.11. Direct fluorescence microscopic analysis for apoptosis induction by AO/EtBr

1 μL of a dye mixture (100 mg/mL acridine orange (AO) and 100 mg/mL ethidium bromide (EtBr), in distilled water) was directly stained with polysaccharides treated cells grown on clean microscope cover slips. After staining the cancer cells were washed with PBS (pH 7.2) and incubated for 1 min, the cells were then visualized under fluorescence microscope (Nikon Eclipse, Inc., Japan) at 400× magnification with an excitation filter at 480 nm.

2.12. Analysis of mitochondrial membrane potential ($\Delta\Psi m$) by Rhodamine 123 staining

Both Siha and LNCap cells were seeded in 6 well plates (1×10^5 cells/well) and allowed to grow for a day before exposed to IC_{50} concentrations of F1 and F2 fractions. After the specific time intervals (24, 48 and 72 h), the cells were fixed in 4% para-formaldehyde, washed twice with PBS, and exposed to the $\Delta\Psi_m$ specific stain Rhodamine 123 (Rh-123) (10 μg/mL) for 30 min at 37 °C. The cells were then washed twice with methanol to remove the excess stain, washed again with PBS, and analyzed for changes in $\Delta\Psi_m$ using fluorescence microscope with an excitation and emission wavelengths of 505 nm and 534 nm, respectively.

2.13. Measurement of DNA damage by DNA fragmentation

DNA damage by apoptosis was evaluated by genomic DNA fragmentation. The cells (1×10^6 cells) were separately suspended in 10 mL of buffer containing 10 mM Tris–HCl and 10 mM EDTA (pH 8.0). The cells were then treated with polysaccharide fractions in 10 mL of a solution containing 10 mM Tris–HCl, 10 mM EDTA (pH 8.0) and 20 mg/mL proteinase K. The mixture was incubated at 37 °C for 3 h, followed by DNA extraction with phenol:chloroform:isoamyl alcohol solution (25:24:1). The extracted DNA was treated with DNase free RNase at a concentration of 20 mg/mL at 4 °C for 45 min and precipitated with 100 mL of 2.5 M sodium acetate and 3 volumes of ethanol. The DNA fragmentation analysis was then carried out by electrophoresis using 10 μg of the extracted DNA from the selected cancer cells for a period of 45 min at 100 V on a 2% agarose gel containing ethidium bromide and visualized under GelDoc System (Alpha Innotech Image Viewer, version 6.0.0, Japan).

2.14. Semi-quantitative RT-PCR analysis for apoptotic gene expression

RT-PCR was performed to determine changes in the expression profiles of bax, bcl-2, p53, cox-2 and β-actin genes. TriZol reagent was used to isolate the total RNA according to the manufacturer's instructions and reverse transcribed. Briefly, the cDNA was synthesized using a cDNA synthesis kit and amplified according to the manufacturers protocols in a 25 μL reaction mixture containing random primer pairs (1.0 μL): 10× buffer (5.0 μL), cDNA (2.0 μg), 25 mM/L MgCl (3.0 μL), 10 mM/L dNTPs (1.0 μL), and Taq polymerase (2.5 U). Semi-quantitative RT-PCR amplification cycles

Table 1
Details of primer sequences used for detection of intrinsic apoptotic gene expression through RT-PCR amplification.

Genes	Primer sequences	Size (bp)
Bax	Forwrd-5′TTTGCTTCAGGGTTTCATCC-3′ Reverse-5′CAGTTGAAGTTGCCGTCAGA-3′	246
bcl-2	Forward-5′-CATCCATTATAAGCTGTCGCA-3′ Reverse-5′-TGCCGGTTCAGGTACTCAGT-3′	498
p53	Forward-5′-GCTCTGAC TGTACCACCATC-3′; Reverse-5′-CTTCTGACGCACACCTATTG-3′	619
cox-2	Forward-5′ GCTGAGCCATACAGCAAATCC-3′ Reverse-5′ GGGAGTCGGGCAATCATCAG-3′	386
β-Actin	Forward-5′ GTTGCTATCCAGGCTGTGC-3′ Reverse-5′ GCATCCTGTCGGCAATGC-3′	540

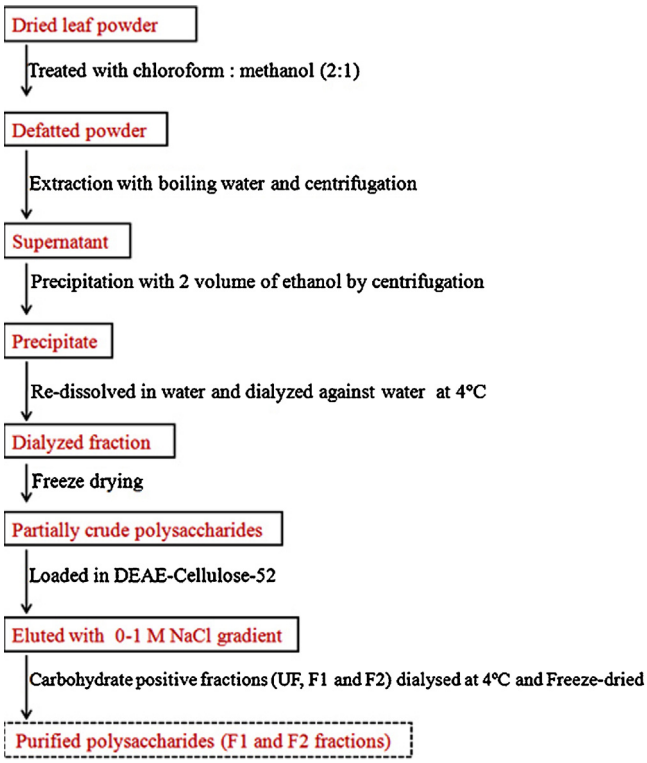

Scheme 1. Steps involved in the extraction and purification of polysaccharides from *C. citratus*.

consisted of denaturation at 94 °C for 1 min, primer annealing at 57 °C for 45 s and extension at 72 °C for 45 s, for a total of 30 cycles followed by final extension at 72 °C for 10 min. The primer sequences are given in Table 1. PCR products were electrophoresed on 1.5% agarose gel containing 0.5 μg/mL EtBr and visualized by transillumination (Alpha Innotech Image Viewer, version 6.0.0, Japan).

2.15. Western blotting analysis

Polysaccharides treated cells were washed in PBS and lysed in 100 μL of buffer containing 50 mM Tris–HCl (pH 8.0), 150 mM NaCl, 1% Triton X-100, 1 mM phenylmethylsulfonyl fluoride, 10 μg/mL pepstatin, and 10 μg/mL leupeptin. After 20 min, extracts were centrifuged at 12,000 rpm for 10 min at 4 °C and supernatants were stored at −80 °C until further use. Proteins (30 μg/lane) were separated using 10% SDS-PAGE, and then transferred to PVDF membranes. Afterwards, the membranes were blocked in TBST solution containing 5% (w/v) non-fat milk for 2 h, followed by overnight incubation at 4 °C with primary antibodies such as caspase 3, cytochrome *c* and β-actin. After being washed with TBST buffer, the membranes were incubated for 1 h with the secondary antibody, horseradish peroxidase-conjugated goat anti-rabbit IgG. Antibody-bound proteins were detected using enhanced chemiluminescence reagents. Blots were washed with washing buffer and incubated with secondary antibodies conjugated with horseradish peroxidase for 1 h at room temperature.

2.16. Statistical analysis

All the experiments were carried out in triplicates and the data were expressed as mean ± SEM. The difference between means was analyzed by one-way ANOVA. All statistical analyses were performed using SPSS 17.0 software. A level of $^{*}p \leq 0.05$, $^{**}p \leq 0.01$ was taken as statistically significant.

3. Results and discussion

3.1. Composition, purity and molecular weight of F1 and F2 fractions of C. citratus

The parameters followed for extraction and purification of the polysaccharides are given in Scheme 1. Crude polysaccharide was isolated from leaves of *C. citratus* through hot water extraction and ethanol precipitation, defatted and dialyzed against water, and freeze dried. The extraction yield of crude polysaccharide was 10.16% of dry mass. The polysaccharide extract was partially purified using anion-exchange chromatography and the profile is shown in Fig. 1a. Chromatogram showed three peaks (A–C), containing active fractions of polysaccharides, were named UF (unbound fraction), F1 and F2 (acidic polysaccharides) respectively and reconstituted separately. The yield and composition of the three fractions were analyzed. The monosaccharide compositions and contents of total sugar, uronic acid and proteins of UF, F1 and F2 fractions are summarized in Table 2. The total sugar content was determined to be 69.4%, 90.98% and 86.12% for these three fractions, using the phenol–sulfuric acid method. The contents of total uronic acid in UF, F1 and F2 fractions were 6.23%, 7.8% and 11.95%, respectively.

All the three fractions (UF, F1 and F2) were subjected to *in vitro* anticancer activity. Among the three fractions, F1 and F2 fractions were observed to exhibit higher anticancer activity against the Siha and LNCap cells than UF fraction. Multiple pharmacological properties of polysaccharides have been reported, and these activities are correlated with their chemical composition and configuration and physical properties. Although it is difficult to explain the structure function correlation of complex polysaccharides, some possible relationships can be inferred. Acidic polysaccharides were found to

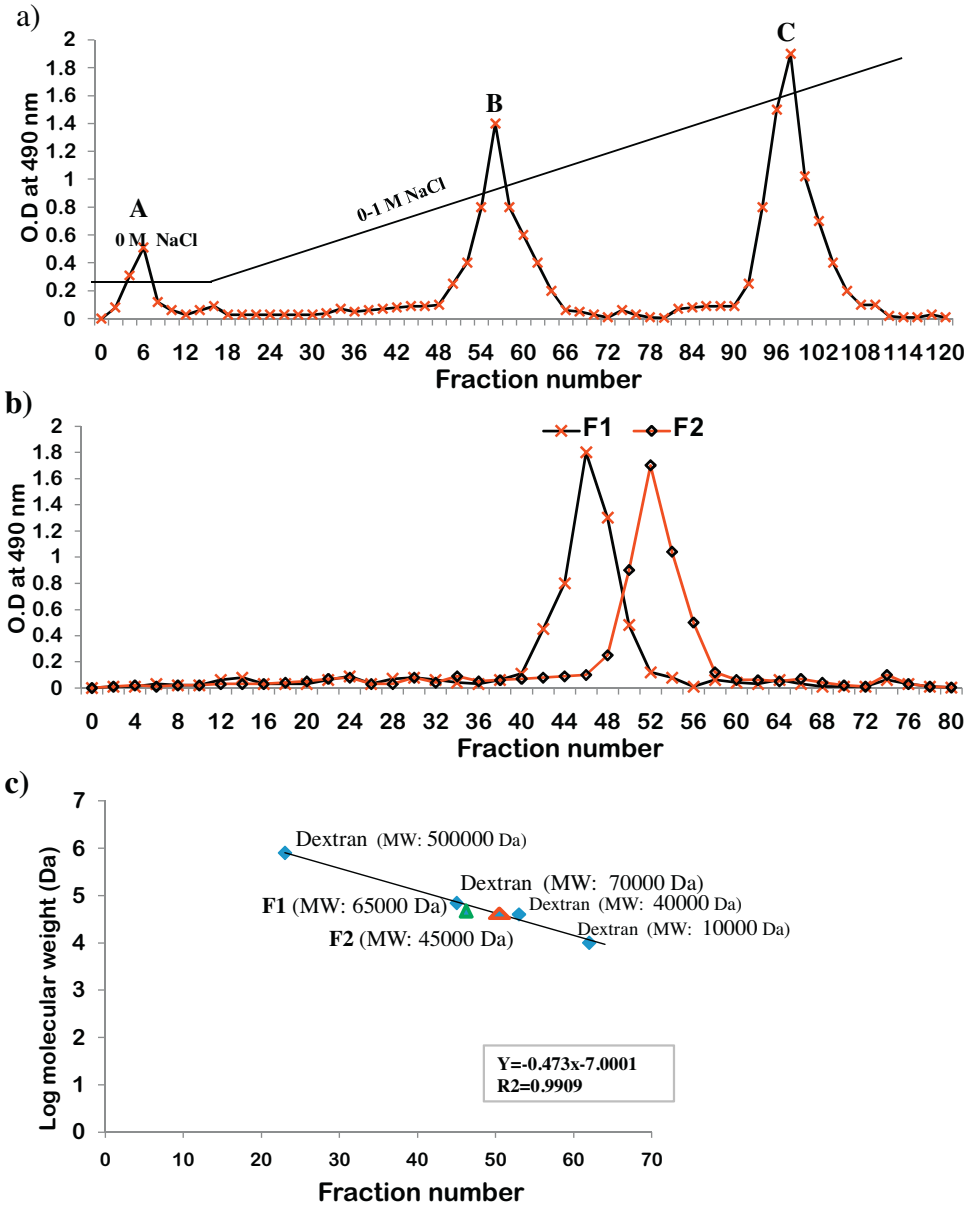

Fig. 1. (a) Anion-exchange chromatography of the crude polysaccharide from *C. citratus* on DEAE-Cellulose 52. The chromatogram shows three peaks (A–C) containing the active polysaccharide fractions. These fractions were named UF (unbound fraction), and F1 and F2 (acidic polysaccharides), respectively. (b) Gel filtration profile of different fractions on Sepharose 6B column chromatography. (c) Gel filtration chromatogram of F1 and F2 polysaccharide fractions; the calibration curve was obtained with dextran standards for molecular weight determination using Sepharose 6B column.

be more biologically active than neutral polysaccharides (Gan, Ma, Jiang, Xu, & Zeng, 2011). The F1 and F2 fractions were subjected to further analysis and composition shown in Table 2. This partially purified polysaccharide F1 and F2 fractions showed a single and relatively symmetrical peak on GPC, indicating its homogeneity (Fig. 1b).

Monosaccharide compositions of F1 and F2 fractions were determined by TFA hydrolysis and HPLC analysis (Fig. 2). HPLC results indicated that the content of xylose in both F1 and F2 fractions was higher than the other monosaccharides such as glucose, galactose and mannose and this suggested that the xylose was the predominant monosaccharide backbone of carbohydrates of these fractions (Fig. 2). Based on the calibration with standard dextrans, the apparent molecular weights of the F1 and F2 fractions were found to be ~65 and ~45 kDa, respectively (Fig. 1c).

Table 2
Yield, composition and molecular weight of UF, F1 and F2 fractions obtained by ion exchange chromatography.

	Yield (% m/m)	Total sugar (% m/m)	Total uronic acid (% m/m)	Total protein (% m/m)	Composition of sugar (% mol)				MW (kDa)
					Glucose	Galactose	Xylose	Mannose	
UF	25.5	69.4	6.23	23.5	–	–	–	–	–
F1	29.8	90.98	7.8	0.5	5.1	11.5	74.5	3.2	~45
F2	39.3	86.12	11.95	0.6	6.2	9.8	69.5	7.3	~65

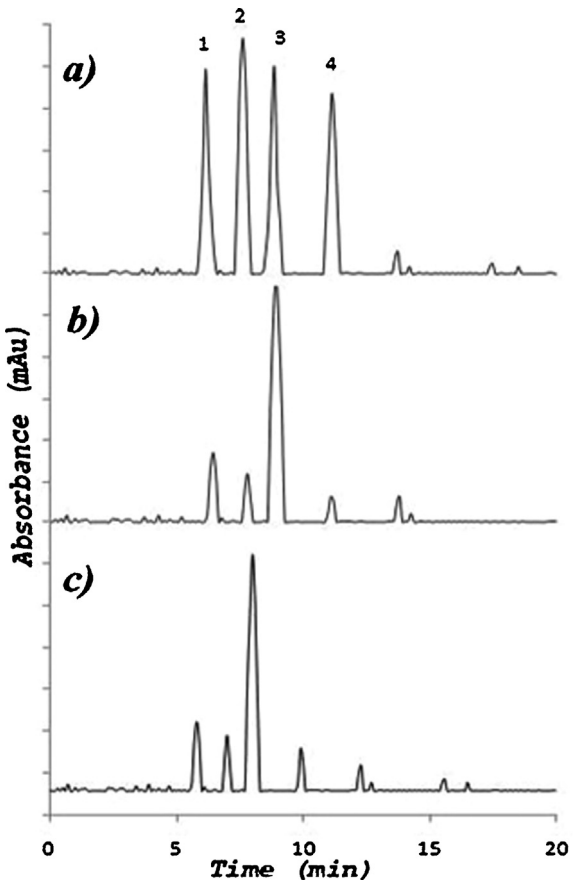

Fig. 2. (a) HPLC profile of standard monosaccharides; peak identity: (1) galatose, (2) glucose, (3) xylose and (4) mannose and (b) hydrolysate of F1, and (c) hydrolysate of F2 fractions.

Molecular weight and monosaccharide composition were also regarded as two important factors related to the anti-cancer activities of polysaccharides (Ooi & Liu, 2000). Chen, Xu, Zhang, and Zeng (2009) reported that polysaccharides with relatively high molecular weight exhibited stronger inhibitory activity against S-180 tumor cells.

3.2. FTIR spectra of F1 and F2 fractions of C. citratus

Fig. 3 illustrates the FTIR spectrum of F1 and F2 polysaccharide fractions of *C. citratus*. The large absorption peak at around 3400 cm^{-1} could be assigned to the stretching vibrations of hydrogen-bonded OH groups. The weak absorption bands at about 3000–2900 cm^{-1} were attributed to C—H stretching vibrations of the free sugar. The strong absorption band at 1610 cm^{-1} was attributed to the C=O asymmetric stretching vibrations of the carboxylate (—COO—) groups. The broad absorption bands with strong intensities at 1420, 1340 and 1240 cm^{-1} could be assigned to deforming vibrations of the C—H bond. The wave numbers between 800 and 1200 cm^{-1} represent the finger print region for carbohydrates (Cui, Phillips, Blackwell, & Nikiforuk, 2007). The absorption bands at about 1180, 1130 and 1010 cm^{-1} were assignable mainly to the C—O—C stretching vibrations and C—O—H bending vibrations. These observations of FTIR analysis further confirmed that F1 and F2 were polysaccharide fractions containing uronic acid.

3.3. NMR spectra of F1 and F2 fractions of C. citratus

The polysaccharide structures of F1 and F2 fractions were investigated by NMR spectroscopy. The ^{1}H and ^{13}C NMR spectra of F1 and F2 fractions recorded in D_2O are given in Table 3 and Fig. 4a–d. The ^{13}C NMR spectrum of F1 fraction showed five main signals at (δ) 102.65 (C-1), 72.67 (C-2), 73.62 (C-3), 76.05 (C-4) and 62.92 (C-5) ppm, which correspond to (1→4) linked b-D-Xyl residues. The kind of signals obtained for ^{13}C NMR spectrum of F2 fraction was similar to that of F1 fraction. The ^{1}H NMR spectrum of F1 fraction showed five main signals at *d* 4.392 (H-1), 3.203 (H-2), 3.469 (H-3), 3.700 (H-4) and 4.013 (H-5) ppm, which correspond to (1→4) linked b-D-Xyl residues. The proton spectrum showed characteristic methyl group signal at 3.377 ppm. The kind of signals obtained for ^{1}H NMR spectrum of F2 fraction was similar to that of F1 fraction. The NMR data for F1 and F2 are reported in Table 3 and Fig. 4a–d,

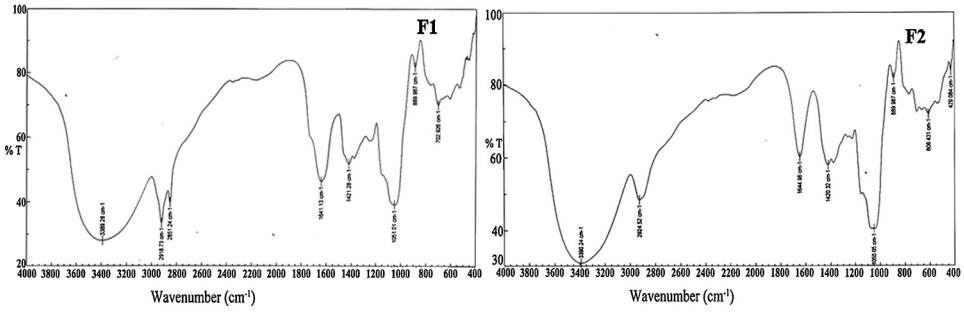

Fig. 3. FTIR spectrum of F1 and F2 in the range of 4000–400 cm^{-1}.

Table 3
Chemical shift (δ) assignments of ^{1}H NMR and ^{13}C NMR spectra of F1 and F2 polysaccharide fractions.

Glycosyl residues		Assigned H, C position				
		1	2	3	4	5
F1 fraction						
→4)-b-D-Xylofuranose-(1→	^{13}C	101.652	72.674	73.626	76.305	62.934
	^{1}H	4.392	3.203	3.469	3.700	4.013
F2 fraction						
→4)-b-D-Xylofuranose-(1→	^{13}C	101.652	72.693	73.644	76.303	62.941
	^{1}H	4.387	3.198	3.464	3.695	4.011

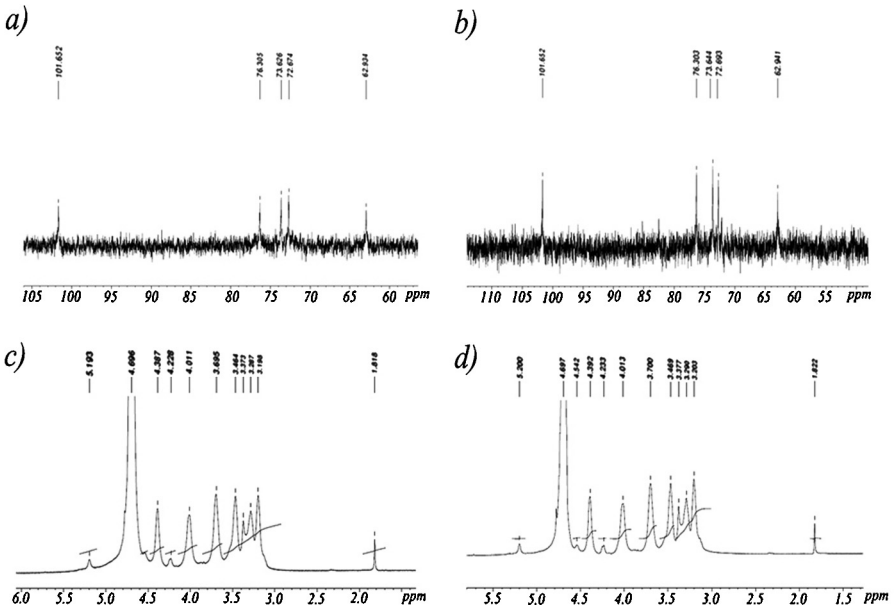

Fig. 4. (a)–(d) ^{1}H and ^{13}C NMR spectra of F1 and F2 polysaccharide fractions.

and are in good agreement with the structures of (1→4) linked b-D-Xylofuranose residues that were described by Habibi, Mahrouz, and Vignon (2005) and Habibi and Vignon (2005).

3.4. Inhibition of cancer cell proliferation in time and dose-dependent manner

In vitro cell toxicity of the polysaccharide fractions UF, F1 and F2 against Siha and LNCap cells was assessed by MTT reduction assay and the results were depicted in Fig. 5. The data revealed noticeable cytotoxicity for all the polysaccharide fractions tested except the UF. The observed cytotoxic effects of the polysaccharide fractions were found to be time- and dose-dependent manner and the cell viability decreased with increasing concentration and incubation duration. The results on cell viability (%) and their IC_{50} concentrations for both Siha and LNCap cells with respect to all the three fractions are depicted in Fig. 5. From Fig. 5, it was observed that F1 and F2 fractions exhibited more significant cytotoxic effect against the cancer cells than UF fractions. Hence, these fractions were taken up for further anticancer studies. Polysaccharides are important components of plants, fungi, yeasts, algae and lichens, and have attracted more and more attention in the biochemical and pharmaceutical fields due to their immuno-modulatory and antitumor effects (Ooi & Liu, 2000; You, Yang, & Lee, 2010). Polysaccharides exhibiting cytotoxic activity on human cancer cells were reported, and few of these polysaccharides showed significant apoptosis-inducing activities in A549 and BL41 cells (Benarba, Meddah, & Aoues, 2012; Lu et al., 2013).

3.5. Induction of apoptosis by fluorescence microscopy analysis

Apoptosis is considered to be the main cell death mechanism that occurs in response to cytotoxicity of the cells. Apoptosis is a tightly regulated process of cellular suicide that is characterized by several morphological and cellular changes including chromatin condensation, membrane blebbing, DNA fragmentation and cleavage of key cellular proteins (Hickman, 1992; Kerr, Winterford, & Harmon, 1994). In this study, we have evaluated the anticancer potential of polysaccharide fractions of *C. citratus* against human reproductive cancer cells such as Siha and LNCap *in vitro* and their possible mechanism of action.

On the basis of overall cell morphology and cell membrane integrity, necrotic and apoptotic cells can be distinguished using fluorescence microscopy. The morphological changes in cells were observed using AO/EtBr fluorescence staining after treating them with F1 and F2 fractions at their IC_{50} concentrations for different incubation duration such as 24 h, 48 h and 72 h (Fig. 6a and b). The images revealed that the apoptotic cells containing the condensed form of nuclei and apoptotic bodies were stained orange

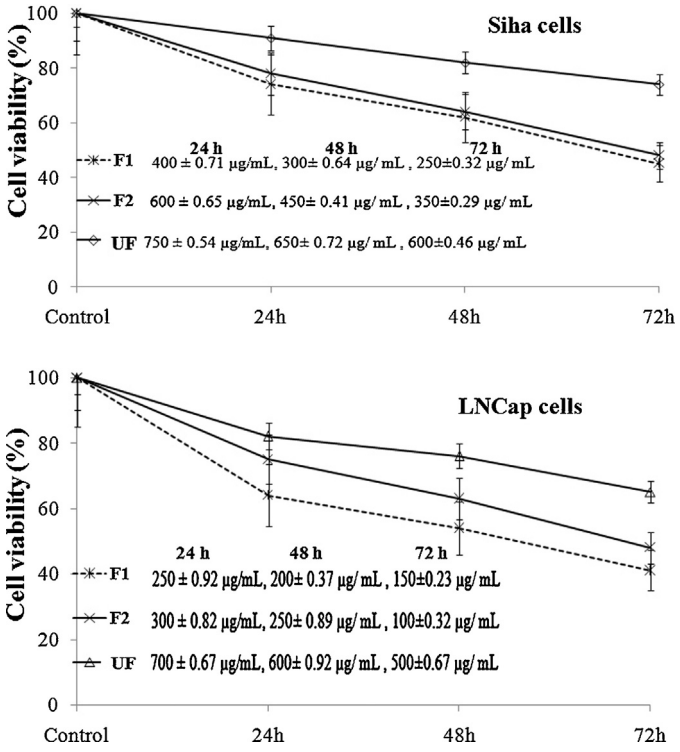

Fig. 5. Polysaccharides fractions (UF (unbound fraction), F1 and F2) attenuated cytotoxicity in Siha and LNCap cancer cells. The cells were treated with F1, F2 and UF in the range of 100–1000 µg/mL for 24 h, 48 h and 72 h. The error bars represent mean values ± SEM of three independent experiments, each performed in triplicates ($p \leq 0.05$). The IC_{50} values are in means ± SD ($n = 3$). $p \leq 0.05$ *vs.* control.

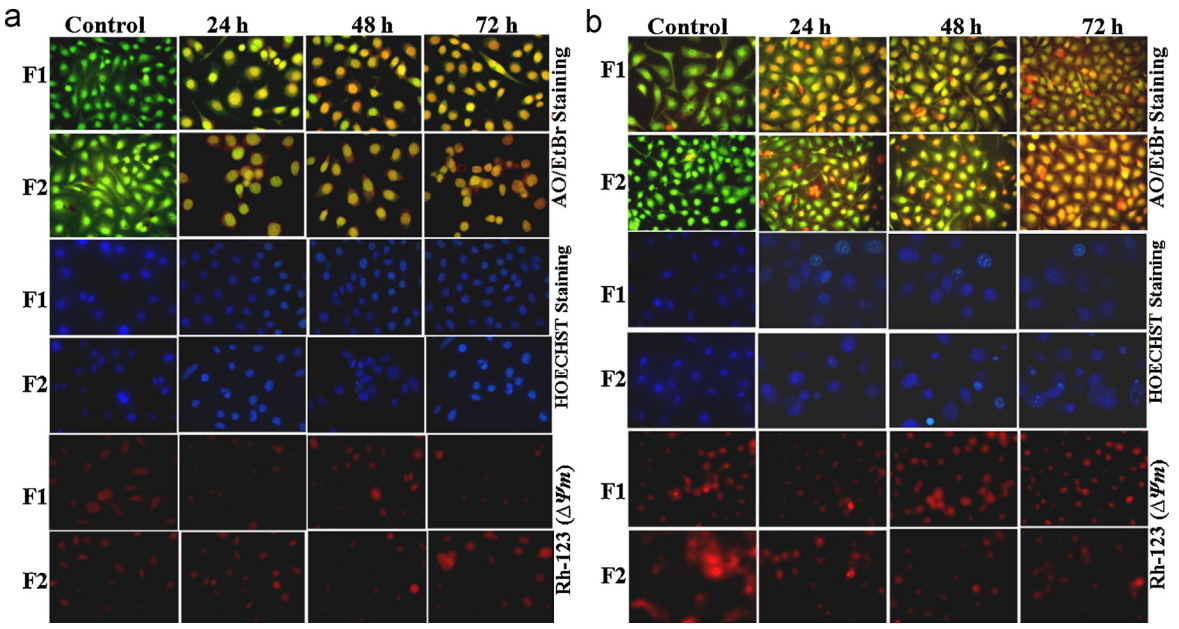

Fig. 6. (a) Fluorescence microscopy images of F1 and F2 polysaccharide fractions on Siha cells. The panel of images shows AO/EtBr staining for induction of apoptosis; HOECHST 33342 staining shows the nuclear fragmentation; Rh-123 staining clearly indicates the loss of mitochondrial membrane potential ($\Delta\Psi_m$). The active mitochondrial membranes are clearly indicated by Rh-123. (b) Fluorescence microscopy images of F1 and F2 polysaccharide fractions on LNCap cells. The panel of images shows AO/EtBr staining for induction of apoptosis; HOECHST 33342 staining shows the nuclear fragmentation; Rh-123 staining clearly indicates the loss of mitochondrial membrane potential ($\Delta\Psi_m$). The active mitochondrial membranes are clearly indicated by Rh-123.

whereas the necrotic cells were stained red and the untreated Siha and LNCap cells were stained uniform green.

Significant differences in apoptosis induction were observed between the control and cancer cells after treatment with F1 and F2 fractions for 24 h, 48 h and 72 h. Though apoptosis was detected in both the cancer cells treated with F1 and F2 fractions, apoptosis induction was higher in cells treated with F1 fraction than F2. The characterization of the cell death induced by F1 and F2 fractions was further examined with the help of fluorescent DNA binding agent, HOECHST 33342. HOECHST 33342 is known to form fluorescent complexes with natural double-stranded DNA and is useful to find out the apoptotic nuclei. Staining with HOECHST 33342 showed the induction of apoptosis upon treatment of cancer cells with the F1 and F2 at their IC_{50} concentrations following exposure for 24 h, 48 h and 72 h whereas control cells (untreated) showed normal cell morphology. Apoptotic nuclei of treated cells were identified by reduced nuclear size, condensed chromatin gathering at the periphery of the nuclear membrane and a total fragmented morphology of nuclear bodies (Fig. 6a and b). The results clearly indicated that the inhibition of growth was induced when the cancer cells were treated with F1 and F2 at their IC_{50} concentrations. Chen et al. (2013) explained the apoptosis of polysaccharide treated BGC-823 cells by means of morphological characteristics such as condensation of chromatin, nuclear pyknosis, formation of apoptotic bodies and nuclear fragmentation using HOECHST and AO/EtBr staining. Therefore, the anti-proliferation effect of F1 and F2 fractions would be associated with their potential to induce apoptosis in the selected cancer cells.

3.6. Analysis of mitochondrial membrane potential ($\Delta\Psi_m$) loss

The mitochondrial membrane potential ($\Delta\Psi_m$) loss of cancer cells was analyzed using the dye, Rh-123 (Fig. 6a and b), and a decrease in mean fluorescence intensity was observed following the treatment of cells with F1 and F2 fractions. The fluorescence images demonstrated the loss of mitochondrial membrane potential ($\Delta\Psi_m$) (Fig. 6a and b) due to mitochondrial membrane depolarization, which was considered to be an initial and irreversible step of apoptosis (Adrie, Bachelet, & Vayssier-Taussat, 2001). The data indicated that the induction of apoptosis in cells by F1 and F2 fractions was accompanied by alterations in the mitochondrial membrane potential ($\Delta\Psi_m$). It was reported that CNE-2

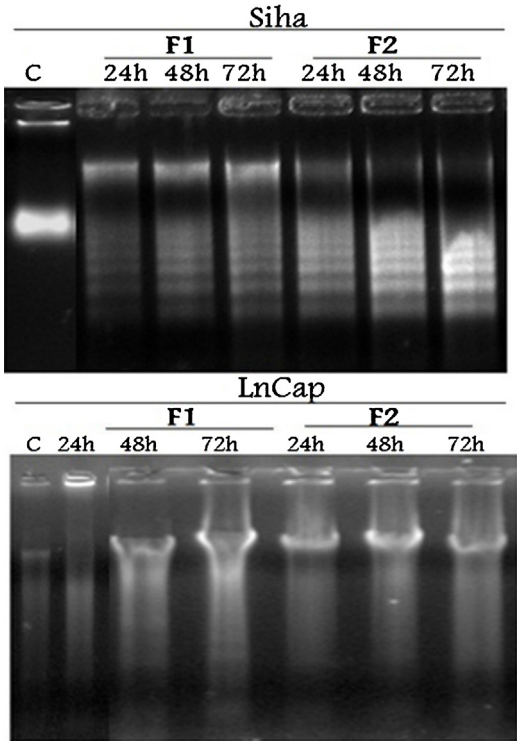

Fig. 7. Polysaccharide fractions induced DNA fragmentation in Siha and LNCap cells. Cells were treated with F1 and F2 for 24 h, 48 h and 72 h. DNA was extracted and analyzed by 2% agarose gel electrophoresis. Both floating and adherent cells were collected, soluble DNA was extracted and electrophoresed on a 2% agarose gel containing 0.05 mg/mL ethidium bromide at 100 V for 45 min. The gels were then photographed under UV illumination. The panel clearly indicates DNA laddering pattern of Siha and LNCap cells.

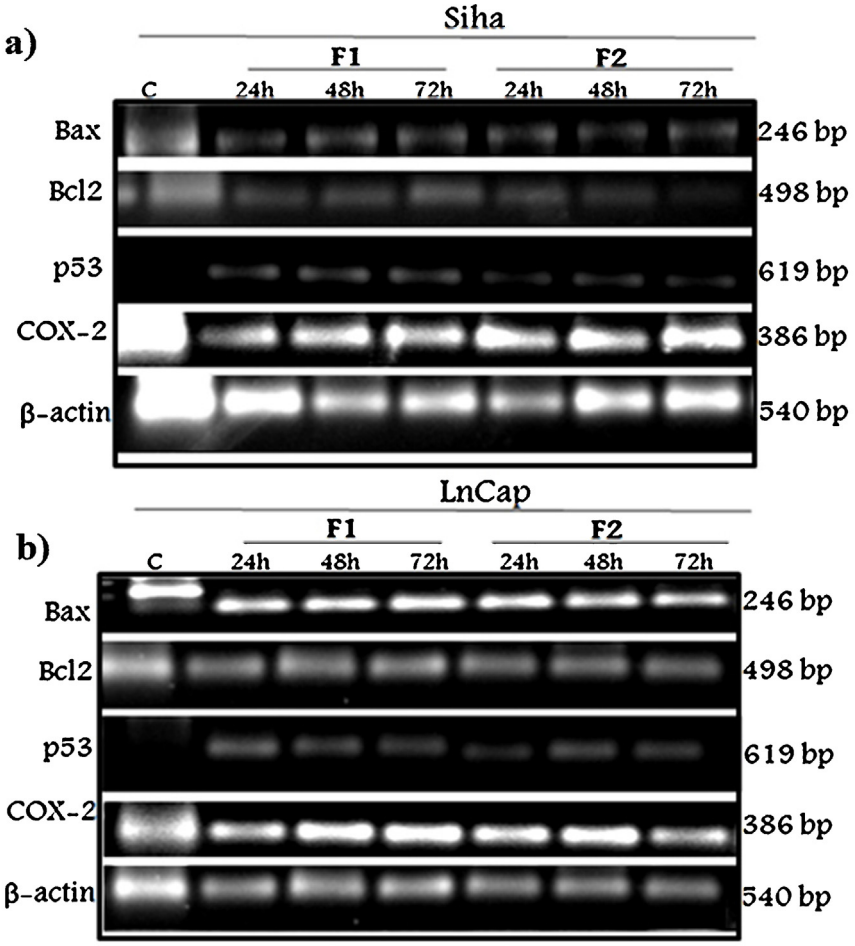
a)
Siha
F1
F2
C
24h
48h
72h
24h
48h
72h
Bax
Bcl2
p53
COX-2
β-actin
246 bp
498 bp
619 bp
386 bp
540 bp
b)
LnCap
F1
F2
C
24h
48h
72h
24h
48h
72h
Bax
Bcl2
p53
COX-2
β-actin
246 bp
498 bp
619 bp
386 bp
540 bp

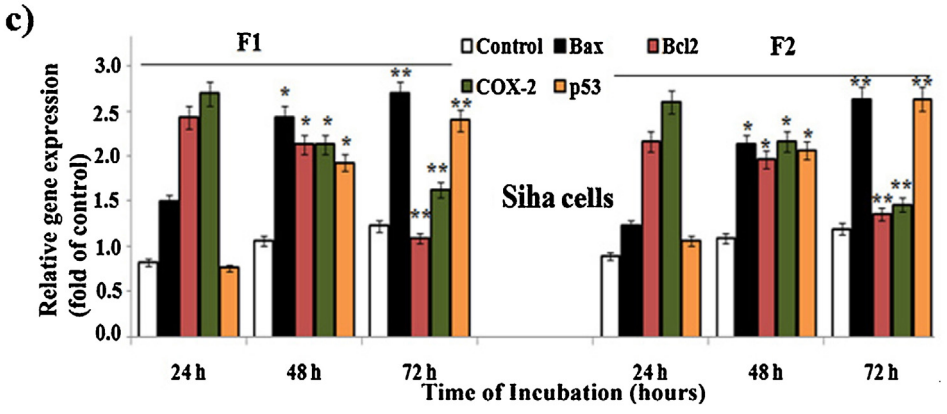
c)
F1
F2
Control
Bax
Bcl2
COX-2
p53
Siha cells
Relative gene expression (fold of control)
3.0
2.5
2.0
1.5
1.0
0.5
0.0
24 h
48 h
72 h
24 h
48 h
72 h
Time of Incubation (hours)

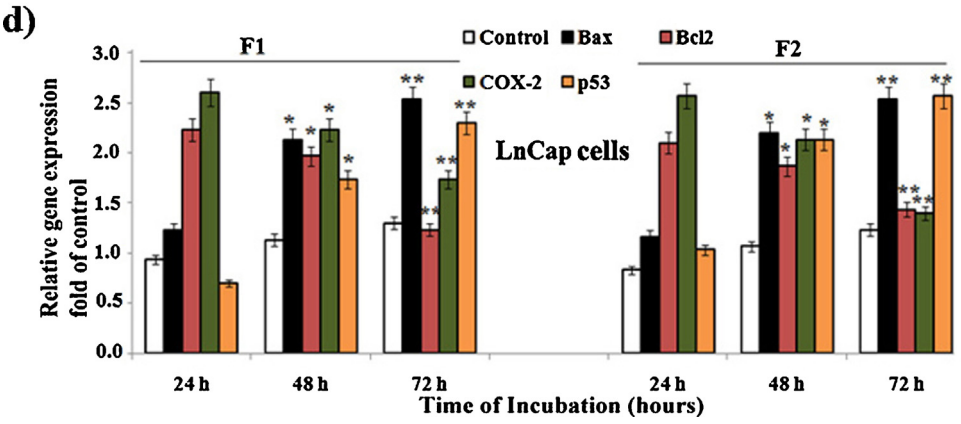
d)
F1
F2
Control
Bax
Bcl2
COX-2
p53
LnCap cells
Relative gene expression fold of control
3.0
2.5
2.0
1.5
1.0
0.5
0.0
24 h
48 h
72 h
24 h
48 h
72 h
Time of Incubation (hours)

cells treated with polysaccharide displayed the characteristic apoptotic morphology. Besides, it was reported that mitochondria played an important role in an intrinsic apoptotic pathway by releasing cytochrome *c*, leading to the activation of the caspase cascade (Gil, Almeida, Oliveira, & Rego, 2003). The results demonstrated that polysaccharide fractions F1 and F2 could disrupt the functions of mitochondria at the early stages of apoptosis, subsequently co-ordinate caspase 3 activation through the cleavage of caspases by the release of cytochrome *c* (Figs. 6 and 9).

3.7. DNA fragmentation analysis

We examined the extent of nuclear DNA fragmentation by agarose gel electrophoresis and the results are shown in Fig. 7. DNA ladder pattern was observed after the treatment of Siha and LNCap cells with F1 and F2. This suggested that these fractions caused DNA fragmentation characteristic of apoptotic process with the generation of multiple DNA fragments and induced apoptosis in these cancer cells at different incubation duration. A biochemical hallmark of apoptosis was the cleavage of chromatin into small fragments including oligonucleosomes, which were described as DNA ladders in the electrophoresed gel (Hu et al., 2010).

3.8. Effect of polysaccharide fractions on markers of intrinsic apoptotic gene expression

To elucidate the apoptotic pathways activated by polysaccharide fractions, semi quantitative RT-PCR and Western blot analyses were carried out to measure the expression of death receptors as well as their corresponding mitotic-mediated apoptotic genes, and bcl-2 family genes. Analysis of the expression of bax, bcl-2, and p53 and cox-2 genes by RT-PCR revealed a significant decrease in the expression of bcl-2 and cox-2 and an increase in the expression of bax and p53 in cells treated with F1 and F2 polysaccharide fractions when compared to untreated control cells (Fig. 8). β-Actin gene was used as an internal house keeping control for the study.

The major gene groups that regulate apoptosis are the bcl-2 family. It has been reported that bcl-2 members (*e.g.*, bcl-2 and p53) protect against multiple signals that lead to cell death whereas bax members (*e.g.*, bax, bad) induce apoptosis. Genes of bcl-2 family regulate a common cell death pathway and function at a point where various signals converge (Hengartner, 2000; Jeong & Seol, 2008). Studies reported that the bcl-2 inhibits cytochrome *c* translocation from the mitochondria to the cytoplasm, thereby blocking the caspase activation step of the mitochondrial mediated-intrinsic apoptotic process (Adams & Cory, 2001, Jiang, Yang, & Cheng, 2004; Han, Kim, & Kim, 2008). The inducible enzyme cox-2 is over-expressed in many cancer cells and suppression of cox-2 gene is associated with the induction of cancer cell apoptosis (Lee et al., 2009; Thangam et al., 2011). Further, it is reported that the expression of cox-2 can be regulated through the PI3K/Akt pathway for the induction of cancer cell apoptosis (Martin et al., 2004; Sheu et al., 2005; Xiao et al., 2013). In the present study, we observed that the polysaccharide fractions dose- and time-dependently down regulated the expression of cox-2 for the induction of bcl-2 family gene expression.

3.9. Analysis of caspase 3 activation for induction of intrinsic apoptotic pathway

In this study, we investigated the involvement of the mitochondrial-mediated intrinsic apoptotic pathway by assessing the release of cytochrome *c* from the mitochondria into the cytoplasm and the cleavage of the caspase 3. As shown in Fig. 9, a significant increase in cytochrome *c* release was observed when Siha and LNCap cells were treated with F1 and F2 polysaccharide fractions, and this release was found to be time- and dose-dependent. We also assessed the expression of tumor suppressor protein p53 using semi quantitative-reverse transcription PCR, and the results showed that F1 and F2 fractions induced apoptotic gene expression in p53-dependent manner as evidenced by increased expression of p53 (Fig. 8a–d). In addition, caspases have been reported to play vital roles in executing apoptosis. To identify the role of caspases involved in the signaling of apoptosis induced by F1 and F2, the Siha and LNCap cells were treated with various IC_{50} concentrations of F1 and F2 for 24 h, 48 h and 72 h. Significant increase in both caspase 9 and cytochrome *c* activities was detected in the treated cells and the increase was found to be in a time-dependent manner as evidenced by the level of expression of internal control protein. The densitometry analysis of apoptotic protein expression profile suggested that polysaccharide fractions F1 and F2 induced apoptosis through the activation of the intrinsic mitochondrial apoptotic pathway in selected cancer cells (Fig. 9a–d).

It is clear that caspase family members play important roles in driving apoptosis (Lavrik, Golks, & Krammer, 2005). Caspase activation appears to be directly responsible for many of the molecular and structural changes in apoptosis. Among the identified caspases, caspase 3 is thought to be the key enzyme that induces apoptosis. The mitochondria-mediated pathway involves the release of cytochrome *c* followed by the formation of apoptosome, activation of caspase 3 and fragmentation of DNA. In order to investigate the mechanism of apoptosis induction in Siha and LNCap cells by F1 and F2 fractions, we assessed the release of cytochrome *c* from the mitochondria into the cytoplasm and examined the role of caspase 3 in cancer cell apoptosis. p53 participates in multiple cellular activities such as cell cycle checkpoints and DNA repair besides playing a critical role in maintaining genome integrity and stability (Hartwell & Weinert, 1989). The activation of p53 and related family members can either enforce cell cycle arrest or induce apoptosis. However, more than half of human tumors are known to display p53 mutation or deficiency (Boatright & Salvesen, 2003). In this current study, we also assessed the expression of p53 in the treated cells and it was observed that the level of p53 expression increased dramatically in the F1 and F2 treatment, which down-regulates the anti-apoptotic factor bcl-2 and up-regulates the pro-apoptotic factor bax.

The accumulation of p53 triggered apoptosis and led to the release of cytochrome *c* from mitochondria to cytosol. Caspase 3 played key roles in the post-mitochondrial apoptotic pathway including the activation of several caspases which are the hallmarks of apoptosis (Boatright & Salvesen, 2003; Zhao et al., 2013). The fractions induced cell death *via* p53 mediated apoptosis, indicating that the polysaccharides may be used as therapeutic agents for tumors with a p53 mutation (Scheme 2).

In conclusion, we demonstrated the efficacy of the acidic polysaccharide fractions F1 and F2 from *C. citrates* for their anticancer activity in Siha and LNCap cells *via* induction of apoptosis. The induction of apoptosis was closely associated with the

Fig. 8. (a) and (b) Semi-quantitative RT-PCR analysis of intrinsic apoptotic related gene expressions of cells treated with F1 and F2 polysaccharide fractions after 24 h, 48 h and 72 h. The treated cells were harvested and analyzed for expression of bcl-2 family genes by RT-PCR. The bands shown here are representative of three independent experiments. β-Actin gene was used as an internal loading control for RT-PCR analysis. (c) and (d) Densitometry analysis of semi-quantitative RT-PCR of intrinsic apoptotic related gene expressions of cells treated with F1 and F2 polysaccharide fractions after 24 h, 48 h and 72 h. The results shown here are representative of three independent experiments. $^{*}p \leq 0.05$ and $^{**}p \leq 0.01$, compared with control groups.

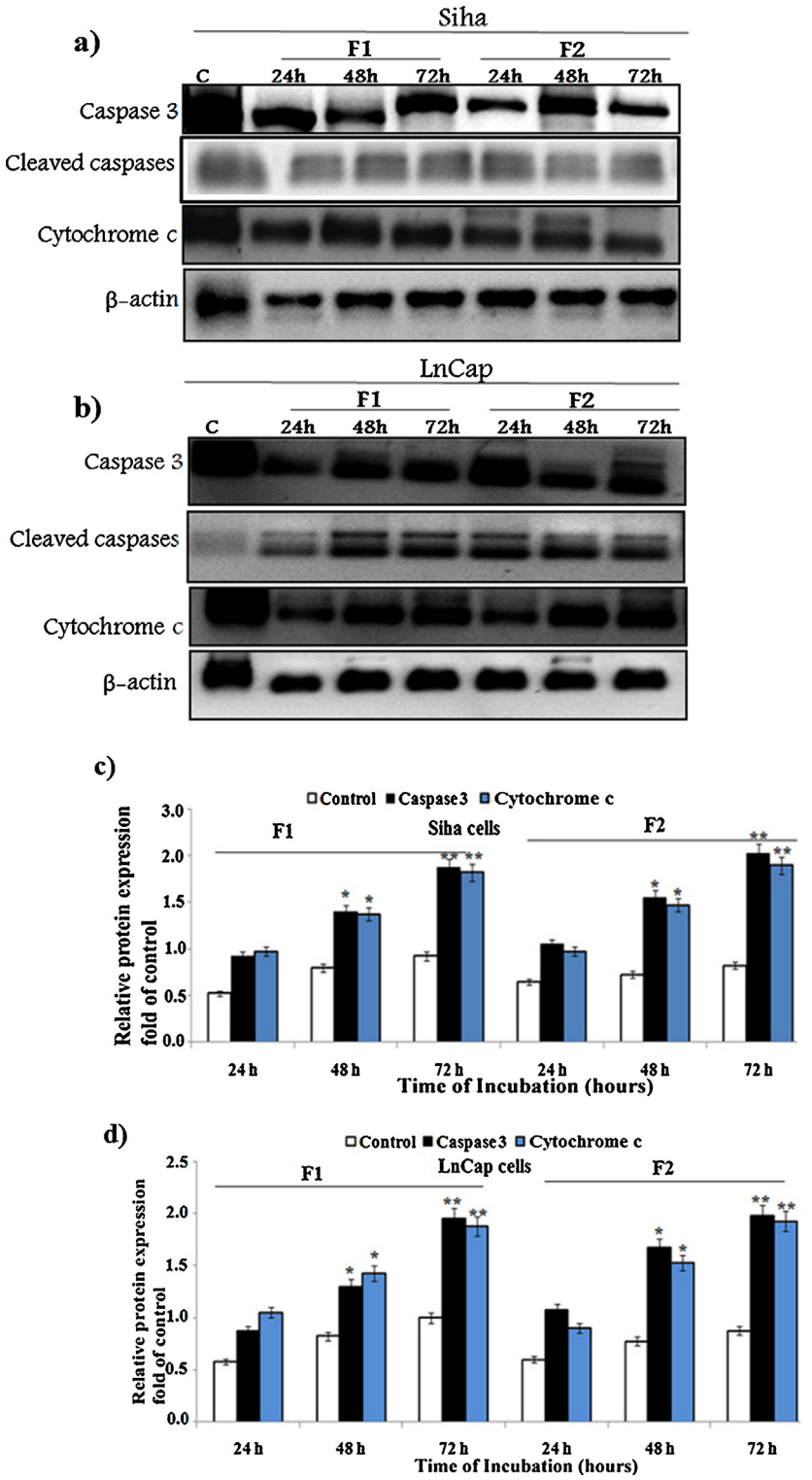

Fig. 9. (a) and (b) Polysaccharide fractions F1 and F2 induced mitochondria dependent apoptosis, wherein the protein expression profile was analyzed by Western blotting at 24 h, 48 h and 72 h. Siha and LNCap cells were treated with their IC_{50} concentrations of F1 and F2, respectively. After 24 h, 48 h and 72 h, the cells were harvested and analyzed for mitochondrial protein expression of the caspase 3 and cytochrome *c* release through cleavage of active caspases by Western blotting. β-Actin was used as an internal control. The blots showed here are representative of three independent experiments. (c) and (d) Densitometry analysis of apoptotic protein expression for F1 and F2 polysaccharide fractions treated cells after 24 h, 48 h and 72 h. The results showed here are representative of three independent experiments. $^{*}p \leq 0.05$ and $^{**}p \leq 0.01$, significantly differs with the control groups.

reduction in mitochondrial transmembrane potential, down-regulation of bcl-2, up-regulation of bax, and activation of caspase 3 in treated cancer cells. The apoptotic signaling pathway involved the events such as loss of mitochondrial membrane potential, release of cytochrome *c* into cytosol, and subsequent activation of caspase 3 cascades responsible for apoptosis. The possible mechanism of apoptosis induction by polysaccharides of the study is illustrated in Scheme 2. Finally, our findings will provide scope for

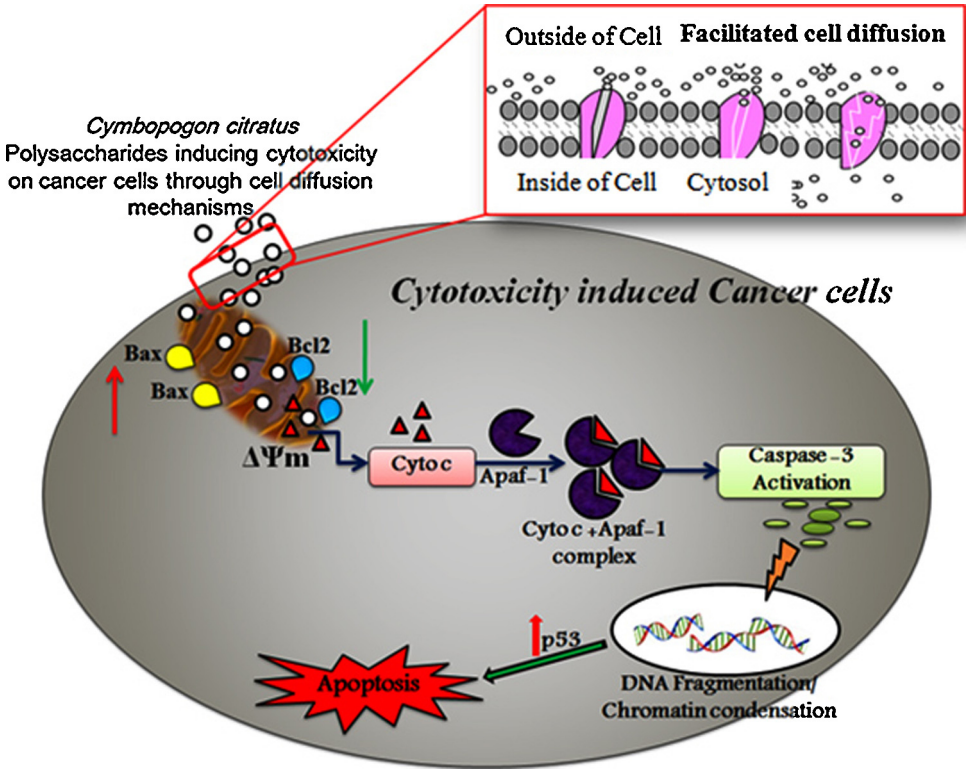

Scheme 2. Possible schematic representations of mechanisms involved in the activation of intrinsic apoptotic signaling pathway in cancer cells by *C. citratus* polysaccharides. The strategy explains the cell diffusing mechanisms of entry of polysaccharides into the cancer cells to induce cytotoxicity.

future studies on polysaccharide based drug development for the treatment of different types of cancers.

Acknowledgements

Authors are very thankful to Dr. P. Gunsekaran, Director (KIPM and R) and Dr. K. Kaveri, Department of Virology, King Institute of Preventive Medicine and Research, Chennai, India for providing necessary facilities to carryout this study. We sincerely express our sincere thanks and gratitude to the Department of Zoology, Bharathiar University, Coimbatore for their constant support during this study.

References

Adams, J. M., & Cory, S. (2001). Life-or-death decisions by the Bcl-2 protein family. *Trends Biochemical Sciences*, *26*, 61–66.

Adrie, C., Bachelet, M., & Vayssier-Taussat, M. (2001). Mitochondrial membrane potential and apoptosis peripheral blood monocytes in severe human sepsis. *Respiratory Critical Care Medicine*, *164*, 389–395.

Benarba, B., Meddah, B., & Aoues, A. (2012). *Bryonia dioica* aqueous extract induces apoptosis through mitochondrial intrinsic pathway in BL41 Burkitt's lymphoma cells. *Journal of Ethnopharmacology*, *141*, 510–516.

Boatright, K. M., & Salvesen, G. S. (2003). Mechanisms of caspase activation. *Current Opinion in Cell Biology*, *15*, 725–731.

Carbajal, D., Casaco, A., Arruzazabala, L., Gonzalez, R., & Tolon, Z. (1989). Pharmacological study of *Cymbopogon citratus* leaves. *Journal of Ethnopharmacology*, *25*, 103–107.

Chen, X., Xu, X., Zhang, L., & Zeng, F. (2009). Chain conformation and anti-tumor activities of phosphorylated (1 → 3)-[beta]-D-glucan from *Poria cocos*. *Carbohydrate Polymers*, *78*, 581–587.

Chen, G., Zhang, P., Huang, T., Yu, W., Lin, J., Li, P., et al. (2013). Polysaccharides from *Rhizopus nigricans* mycelia induced apoptosis and G2/M arrest in BGC-823 cells. *Carbohydrate Polymers*, *97*, 800–808.

Costa, C. A. R., Kohn, D. O., Lima, V. M., Gargano, A. C., Flório, J. C., & Costa, M. (2011). The GABAergic system contributes to the anxiolytic-like effect of essential oil from *Cymbopogon citratus* (lemongrass). *Journal of Ethnopharmacology*, *137*, 828–836.

Cui, S. W., Phillips, G. O., Blackwell, B., & Nikiforuk, J. (2007). Characterisation and properties of Acacia senegal (L.) Willd. var. senegal with enhanced properties (Acacia (sen) SUPERGUM™): Part 4. Spectroscopic characterisation of Acacia senegal var. senegal and Acacia (sen) SUPERGUM™ arabic. *Food hydrocolloids*, *21*(3), 347–352.

Dubois, M., Gilles, K. A., Hamilton, J. K., Rebers, P. A., & Smith, F. (1956). Colorimetric method for determination of sugars and related substances. *Analytical Chemistry*, *28*, 350–356.

Filisetti-Cozzi, T. M. C. C., & Carpita, N. C. (1991). Measurement of uronic acids without interference from neutral sugars. *Analytical Biochemistry*, *197*, 157–162.

Francisco, V., Figueirinha, A., Neves, B. M., Rodríguez, C. G., Lopes, M. C., Cruz, M. T., et al. (2011). Cymbopogon citratus as source of new and safe anti-inflammatory drugs: Bio-guided assay using lipopolysaccharide-stimulated macrophages. *Journal of Ethnopharmacology*, *133*, 818–827.

Gan, D., Ma, L., Jiang, C., Xu, R., & Zeng, X. (2011). Production, preliminary characterization and antitumor activity *in vitro* of polysaccharides from the mycelium of *Pholiota dinghuensis* Bi. *Carbohydrate Polymers*, *84*, 997–1003.

Gil, J., Almeida, S., Oliveira, C. R., & Rego, A. C. (2003). Cytosolic and mitochondrial ROS in staurosporine-induced retinal cell apoptosis. *Free Radical Biology & Medicine*, *35*, 1500–1514.

Habibi, Y., Mahrouz, M., & Vignon, M. R. (2005). D-Xylans from seed endosperm of *Opuntia ficus-indica* prickly pear fruits. *Comptes Rendus Chimie*, *8*, 1123–1128.

Habibi, Y., & Vignon, M. R. (2005). Isolation and characterization of xylans from seed pericarp of *Argania spinosa* fruit. *Carbohydrate Research*, *340*, 1431–1436.

Han, S. I., Kim, Y. S., & Kim, T. H. (2008). Role of apoptotic and necrotic cell death under physiologic conditions. *BMB Reproduction*, *41*, 1–10.

Hartwell, L., & Weinert, T. (1989). Checkpoints: Controls that ensure the order of cell cycle events. *Science*, *246*, 629–634.

Hengartner, M. O. (2000). The biochemistry of apoptosis. *Nature*, *407*, 770–776.

Hickman, J. A. (1992). Apoptosis induced by anticancer drugs. *Cancer Metastasis Reviews*, *11*, 121–139.

Hu, T. J., Wei, X., Zhang, X., Cheng, F. S., Shuai, X. H., Zhang, L., et al. (2010). Protective effect of *Potentillaanserine* polysaccharide (PAP) on hydrogen peroxide induced apoptosis in murine splenic lymphocytes. *Carbohydrate Polymers*, *79*, 356–361.

Jeong, S. Y., & Seol, D. W. (2008). The role of mitochondria in apoptosis. *BMB Reproduction*, *41*, 11–22.

Jiang, C., Yang, Y. F., & Cheng, S. H. (2004). Fas ligand gene therapy for vascular intimal hyperplasia. *Current Gene Therapy*, *4*, 33–39.

Kerr, J. F. R., Winterford, C. M., & Harmon, B. V. (1994). Apoptosis: Its significance in cancer and cancer therapy. *Cancer*, *73*, 2013–2016.

Lavrik, I. N., Golks, A., & Krammer, P. H. (2005). Caspases: Pharmacological manipulation of cell death. *Journal of Clinical Investigation*, *115*, 2665–2672.

Lee, K. S., Lee, H. J., Ahn, K. S., Kim, S. H., Nam, D., Kim, D. K., et al. (2009). Cyclooxygenase-2/prostaglandin E_2 pathway mediates icariside II induced apoptosis in human PC-3 prostate cancer cells. *Cancer Letters*, *280*, 93–100.

Lines, A. C. (1996). High-performance liquid chromatographic mapping of the oligosaccharides released from the humanized immunoglobulin, CAMPATHTM1H. *Journal of Pharmaceutical and Biomedical Analysis*, *14*, 601–608.

Lorenzetti, B. B., Souza, G. E., Sarti, S. J., Filho, D. S., & Ferreira, S. H. (1991). Myrcene mimics the peripheral analgesic activity of lemongrass tea. *Journal of Ethnopharmacology*, *34*, 43–48.

Lu, X., Liu, W., Wu, J., Li, M., Wang, J., Wu, J., et al. (2013). A polysaccharide fraction of adlay seed (*Coixlachryma-jobi* L.) induces apoptosis in human non-small cell lung cancer A549 cells. *Biochemical and Biophysical Research Communications*, *430*, 846–851.

Martin, D., Rojo, A. I., Salinas, M., Diaz, R., Gallardo, G., Alam, J., et al. (2004). Regulation of heme oxygenase-1 expression through the phosphatidylinositol 3-kinase/Akt pathway and the Nrf2 transcription factor in response to the antioxidant phytochemical carnosol. *Journal of Biological Chemistry*, *279*, 8919–8929.

Mosman, T. (1983). Rapid colorimetric assay for cellular growth and survival: Application to proliferation and cytotoxicity assays. *Journal of Immunological Methods*, *65*, 55–63.

Negrelle, R. R. B., & Gomes, E. C. (2007). *Cymbopogon citratus* (DC.) Stapf: Chemical composition and biological activities. *Revista Brasileira de Plantas Medicinais*, *9*, 80–92.

Ooi, V. E., & Liu, F. (2000). Immunomodulation and anti-cancer activity of polysaccharide–protein complexes. *Current Medicinal Chemistry*, *7*, 715–729.

Sheu, M. L., Ho, F. M., Yang, R. S., Chao, K. F., Lin, W. W., Lin-Shiau, S. Y., et al. (2005). High glucose induces human endothelial cell apoptosis through a phosphoinositide 3-kinase-regulated Cyclooxygenase-2 pathway. *Arteriosclerosis Thrombosis and Vascular Biology*, *25*, 539–545.

Thangam, R., Soundarapandian, K., Babu, S., Palani, G., Krishnasamy, K., Sambasivam, M., et al. (2011). Over expression of cyclooxygenase 2 detected in MCF-7 breast cancer cell and compared with lung carcinoma cellline (A549). *International Journal of Biomedical Research*, *2*, 320–333.

Thangam, R., Suresh, V., & Kannan, S. (2014). Optimized extraction of polysaccharides from *Cymbopogon citratus* and its biological activities. *International Journal of Biological Macromolecules*, http://dx.doi.org/10.1016/j.ijbiomac.2014.01.033

Xiao, H., Wang, J., Yuan, L., Xiao, C., Wang, Y., & Liu, X. (2013). Chicoric acid induces apoptosis in 3T3-L1 preadipocytes through ROS-mediated PI3K/Akt and MAPK signaling pathways. *Journal of Agricultural and Food Chemistry*, *61*,1509–1520.

Xin, G., Zhaohui, Z., Wenjing, S., & Changhu, X. (2011). Determination of glycosaminoglycan in sea cucumber by HPLC with post column derivatization. *Mathematical and Physical Fisheries Science*, *9*, 105–114.

Yang, X. B., Zhao, Y., & Wang, H. F. (2005). An composition analysis of angelica polysaccharide by high-performance liquid chromatography with post column derivatization. *Chinese Journal of Analytical Chemistry*, *33*,1287–1290.

You, S. G., Yang, C., & Lee, H. Y. B. Y. (2010). Molecular characteristics of partially hydrolyzed fucoidans from sporophyll of *Undaria Pinnatifida* and their *in vitro* anticancer activity. *Food Chemistry*, *119*, 554–559.

Zhao, R., Gao, X., Cai, Y., Shao, X., Jia, G., Huang, Y., et al. (2013). Antitumor activity of *Portulaca oleracea* L. polysaccharides against cervical carcinoma *in vitro* and *in vivo*. *Carbohydrate Polymers*, *96*, 376–383.